

Multiple Fault Detection of Induction Motors with Zero Crossing Time (ZCT)

Abdülkadir Çakir, Eyüp Çaki

Faculty of Engineering, Department of Computer Engineering, Suleyman Demirel University, Isparta, Turkey

ABSTRACT

Induction motors are motion mechanisms used in almost every area of the industrial sector, including daily life. In this study; In the fault detection of induction motors, rotor failure, mechanical unbalance (variable load) failure and mains unbalance fault, also mains unbalance and rotor fault, mechanical unbalance and rotor fault, mechanical unbalance and mains unbalance, mechanical unbalance network unbalance and rotor fault are examined together. Detection of these faults was carried out using ZCT signal in Matlab/Simulink environment.

KEYWORDS: Induction Motor, Fault, Rotor, Network Unbalance, Mechanical Unbalance, Simulink, ZCT, Zero Crossing Time

How to cite this paper: Abdülkadir Çakir | Eyüp Çaki "Multiple Fault Detection of Induction Motors with Zero Crossing Time (ZCT)" Published in International Journal of Trend in Scientific Research and Development (ijtsrd), ISSN: 2456-6470, Volume-6 | Issue-4, June 2022, pp.960-967, URL: www.ijtsrd.com/papers/ijtsrd50215.pdf



Copyright © 2022 by author(s) and International Journal of Trend in Scientific Research and Development Journal. This is an Open Access article distributed under the terms of the Creative Commons Attribution License (CC BY 4.0) (<http://creativecommons.org/licenses/by/4.0>)



1. INTRODUCTION

In the detection of electrical faults in induction motors; current, voltage, vibration, temperature and velocity signals are used (Calis & Caki, 2014; Tao et al., 2021; Tran, Liang, Li, & Pham, 2021; Ukil, Chen, & Andenna, 2011). In this study, fault detection was performed using ZCT signal without using an additional sensor.

Rotor, mechanical unbalance and mains unbalance faults that occur in induction motors are based on the study. These faults cause the change of magnetic flux density. This change caused by the faults causes the formation of new and different amplitude harmonics in the stator current and ZCT. These newly formed components or the amplitude changes in existing components are used as parameters in fault monitoring. In the literature studies, the fault detection method is found from the amplitude of the f component in the stator current of the motor (1-2s). Since this amplitude value is very close to f , it is difficult to detect. As the load of the engine increases, the sensitivity of the method increases, but with the ZCT method, the failure of the engine can be detected even at very small loads. Due to the problems experienced in the detection of faults from the motor

current, fault detection with the ZCT method was preferred.

2. OBTAINING THE ZCT SIGNAL

ZCT data is generated from the series of values obtained from the zero-crossing moments of each phase of the three-phase induction motor. Each stator phase current passes through zero twice in a period, a total of 6 zero crossing points are formed for the three phases. The ZCT data is obtained from the difference in time at the moments of two consecutive zero-crossings (Equation 1). If the induction motor is fed from a balanced network, the motor windings are symmetrical, running at constant load and speed, the zero transition moments occur at 60° intervals along the time axis and the ZCT change is zero. Since a phase passes through zero twice in a period in a 50 Hz system, it passes through a total of 300 zeros, $2 \times 3 \times 50$ for three phases (Figure 1). It is not possible to find an ideal network and symmetrically wound motor in real life, ZCT data contains a wealth of information reflecting internal and external conditions (Askari, Keivani, Ganbariyan, & Kavehnia, 2007; Çalış & Çakır, 2007).

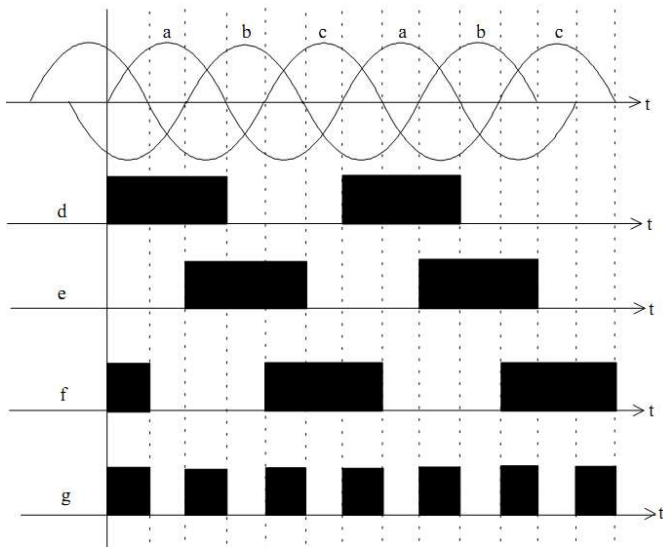


Figure 1. Obtaining ZCT data from three phase stator current

The block diagram of the circuit that obtains the ZCT signal is shown in Figure 2. The amplitudes of the three-phase stator current value are reduced with the current sensor and applied to the op-amps working as a comparator. A square wave at the "TTL" level is obtained from the output of the comparator op-amp used for each phase. Digitized output of each phase is multiplied with "AND" gates as a binary group and summed by applying "OR" gate. In Figure 1, a, b, c shows the outputs of the current sensors, d, e, f shows the outputs of the op-amp comparator, and g shows the waveform resulting from the collection of square waves with logic gates. By inverting the ZCT signal with the 7404 IC, the time difference between one zero crossing point and the next zero crossing point can be determined. The ZCT values of a motor fed from a 50 Hz balanced network and whose motor windings are symmetrical are 3333µs (the time that logically passes from 1 to 0). This value varies between 1 and 3333µs due to the deterioration of symmetry in the motor windings and changes in the network.

$$ZCT_n = T_n - T_{n-1} \quad (1)$$

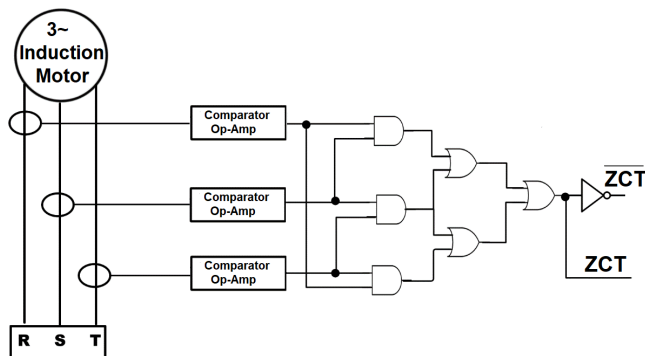


Figure 2. Block diagram of fault detection mechanism of three-phase induction motor with ZCT method

2.1. Characteristics of ZCT Signal

Current studies in induction motor sensorless fault detection use the voltage applied to the motor and the stator current. This method requires fast and high resolution sampling of current and voltage values. If the current or voltage value of three phases is sampled at the same time, an additional analog-to-digital converter (ADC) is needed. This increases the hardware and increases the cost. The ZCT method is a cheaper, sensitive and sensorless fault detection method than the current sampling method with ADC (Çalış & Çakır, 2007; Taleb, Debnath, & Patterson, 2005).

The reason for choosing the ZCT method in the study is that the samples are not affected by the amplitude of the mains voltage, do not require additional sensors, can be used in hazardous environments for humans, and are simple and inexpensive.

3. SIMULATION OF INDUCTION MOTOR FAULTS

The model in Figure 3 was used in the Matlab/Simulink program to simulate the induction motor errors. A 4-pole motor with a power of 4 kW is used in the model. There are 3 main malfunctions, these are rotor, mechanical imbalance and network imbalance. Fault indicators were determined by modeling single, double and triple combinations of each fault (Figure 4).

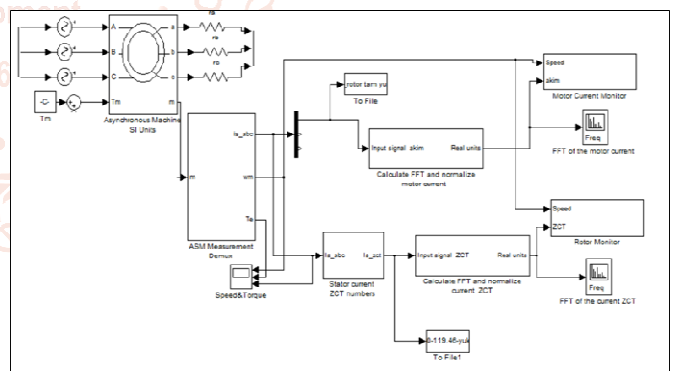


Figure 3. Matlab/Simulink model used to simulate induction motor failures

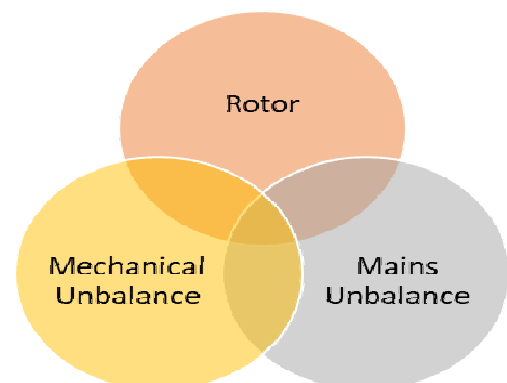


Figure 4. Single, double and triple combinations of faults

3.1. Rotor Failure Modeling and Feature Extraction with Matlab/Simulink

Deformations and breaks in the rotor bars change the rotor resistance. Since the rotor bars are connected in parallel to each other, the deformation and breakage of a bar affects the total rotor resistance. In the model in Figure 3, rotor resistance is added to simulate rotor failure. Rotor error was created by increasing the value of one of the rotor resistances from 0.1Ω to 0.205Ω in 0.0175Ω steps. In the model, the FFT of the ZCT change was calculated and the values in the amplitude of the component were examined. The amplitude variation of the components in the sidebands of the network frequency was investigated by operating the model at quarter, half and full load, and it is seen that the rotor error is in the $2sf$ component in the ZCT signal (Figure 5). In the current signal, it is observed that it is in $(1-2s)f$ and $(1+2s)f$ components, but when this component is very close to the network frequency and the slip (s) is very small, fault detection is difficult (Figure 6).

As can be seen in Figure 5a and Figure 6a, the change of components cannot be observed in the case of no-load operation. Figure 5. In b and Figure 6b, the motor operates at low loads. In Figure 6b, it is difficult to detect because the $(1\pm 2s)f$ component of the current signal is very close to the grid frequency. In Figure 5b, the $2sf$ component appears in the ZCT method. The absence of large amplitude components around the $2sf$ component facilitates fault discrimination.

When the amount of load in the motor increases, it becomes easier to detect the rotor failure from the current signal (Figure 6c and d). In the ZCT method, when the amount of load increases, the detection of rotor failure becomes easier (Figure 5c and d).

In Figure 7, the ZCT spectrum of the full load condition, 1, 2 and 3 rotor bars broken is shown. Likewise, under full load, the current spectra of the solid state, 1, 2 and 3 rotor bars are broken (Figure 8). In the motor operating at full load, the increase in the number of broken rods in the rotor ($1\pm 2s$) causes small changes in the amplitude of the f component, while the increases in the amplitude of the $2sf$ component are evident. As seen in Figure 7, the rotor fault level can be determined from the amplitude of the $2sf$ component of the ZCT signal.

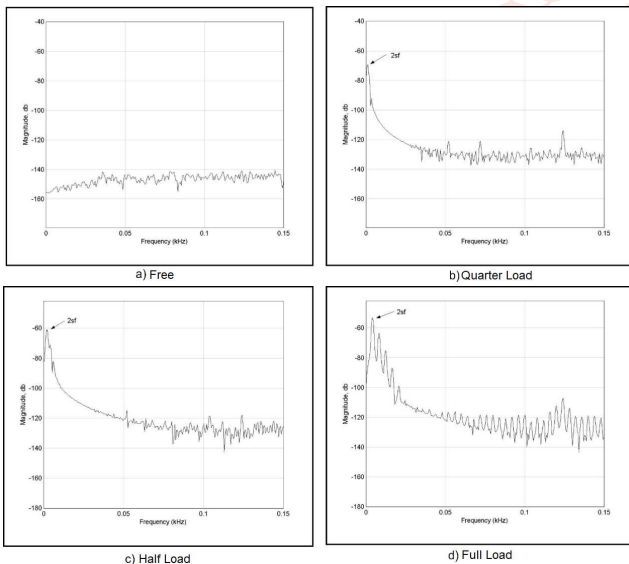


Figure 5. ZCT spectra of rotor error at idle, quarter, half and full load conditions

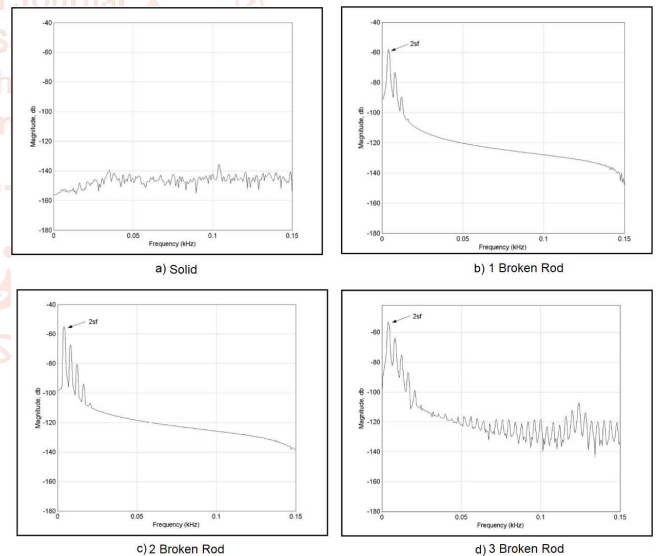


Figure 7. ZCT spectra of the motor at full load, solid, 1, 2 and 3 broken rod states

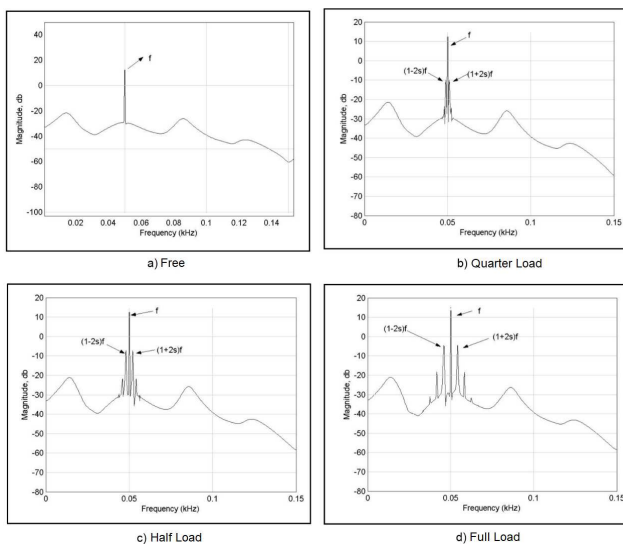


Figure 6. Current spectra of rotor fault at idle, quarter, half and full load conditions

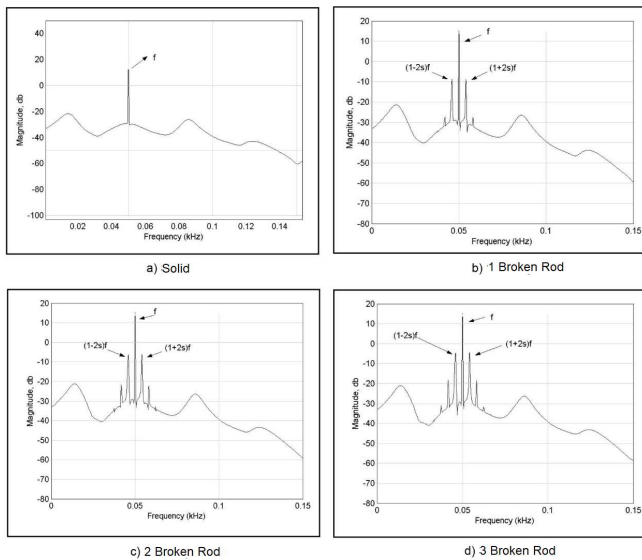


Figure 8. Current spectra of the motor at full load, solid, 1, 2 and 3 broken rod states

3.2. Modeling and Feature Extraction of Mechanical Unbalance (Variable Load) Failure with Matlab/Simulink

The 4-pole induction motor with a power of 4 kW was used as a basis for modeling the mechanical unbalance failure. In the realized model, the load was made variable and applied to the engine as quarter, half or full load. The components in the sidebands of the network frequency are examined and it is seen that the mechanical unbalance fault is in the f_r component of the ZCT signal. It has been observed that the current signal is also in the f_r component. In Figure 9, the ZCT and current spectrums of the engine at quarter load (28+2.8sin155t Nm) are shown. The ZCT and current spectra of the half-loaded state in Figure 10 and the full-loaded state in Figure 11 are shown. It has been determined that the rotor failure and the mechanical imbalance are in different components, and it can be distinguished when the two faults occur simultaneously.

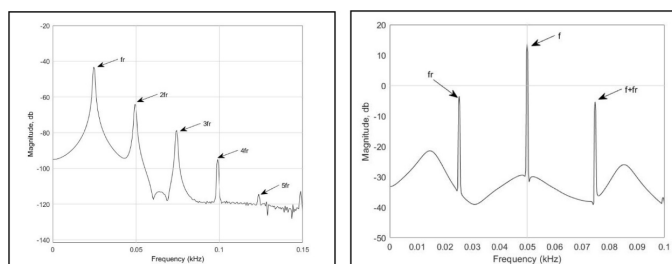


Figure 9. ZCT spectra for quarter load condition with motor mechanical unbalance and current spectrums for quarter load condition with mechanical unbalance of the motor

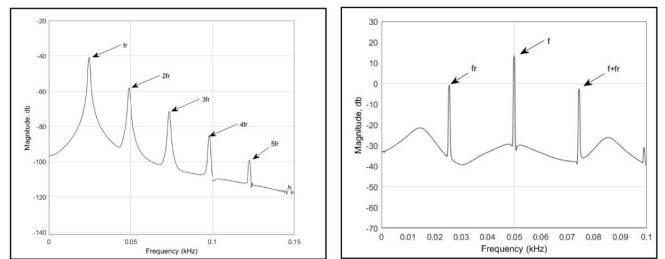


Figure 10. ZCT spectra for half load condition with motor mechanical unbalance and current spectrums for half load condition with mechanical unbalance of the motor

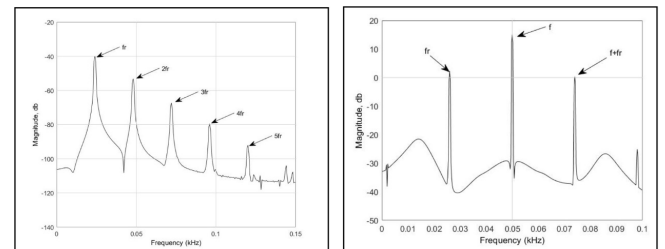


Figure 11. ZCT spectra for full load condition with mechanical unbalance of the motor and current spectrums for full load condition with mechanical unbalance of the motor

3.3. Network Imbalance Modeling and Feature Extraction with Matlab/Simulink

The 4-pole induction motor with a power of 4 kW was used as the basis for modeling the grid unbalance. In the realized model, the mains voltage was applied to the motor at a quarter, half and full load by 3%, starting from 0.5% and increasing in 0.5% steps. As a result of the investigations, it has been determined that the network unbalance is in the amplitude of the $2f$ component in the ZCT signal and in the amplitude of the $3f$ component in the current signal. Mains unbalance, mechanical unbalance and rotor faults occur in different components and are not affected by each other. Figure 12 shows the ZCT and current spectrums at motor quarter load and at 1.5% grid unbalance. In Figure 13, ZCT and current spectrums are shown in case the motor is at half load and the mains unbalance is 1.5%. In Figure 14, the ZCT and current spectrums are seen at full load of the motor and the mains unbalance is 1.5%. When the network unbalance ratio is 3%, ZCT and current spectrums for quarter, half and full load situations are shown.

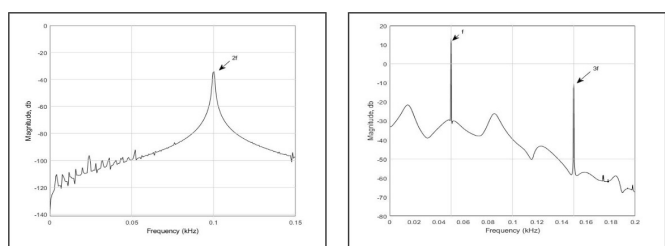


Figure 12. ZCT spectra for a quarter load condition with a grid unbalance of 1.5% and current spectrums for a quarter-load condition where the grid unbalance is 1.5%

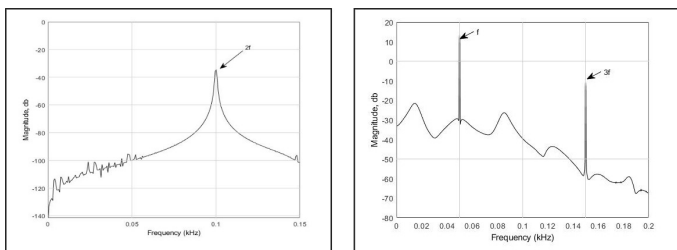


Figure 13. ZCT spectra for half load condition with 1.5% grid unbalance and current spectrums for half load condition with 1.5% mains unbalance

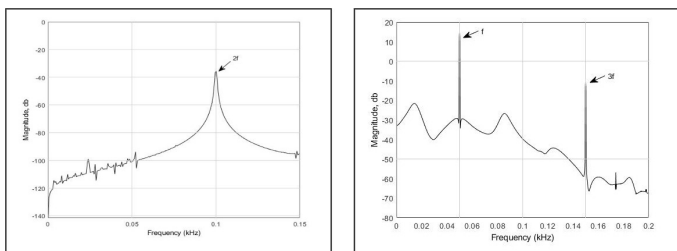


Figure 14. ZCT spectrums for full load condition with 1.5% grid unbalance and current spectrums for full load condition with 1.5% mains unbalance

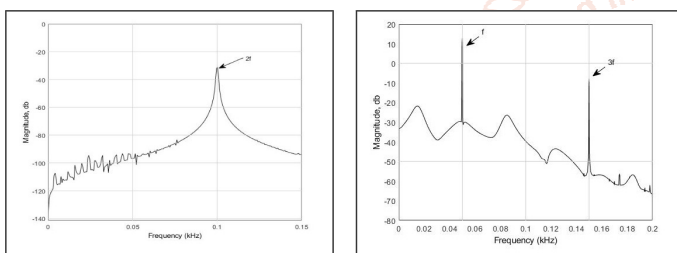


Figure 15. ZCT spectra for quarter load condition with 3% grid unbalance and current spectrums for quarter load condition with 3% grid unbalance

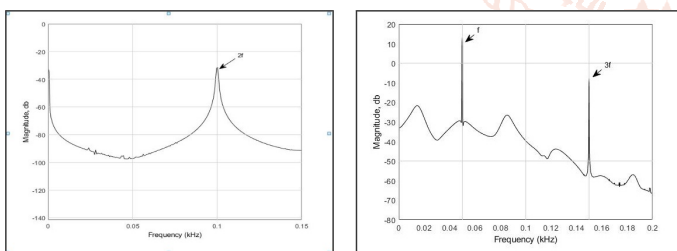


Figure 16. ZCT spectrums for half load condition with 3% grid unbalance and current spectrums for half load condition with 3% grid unbalance

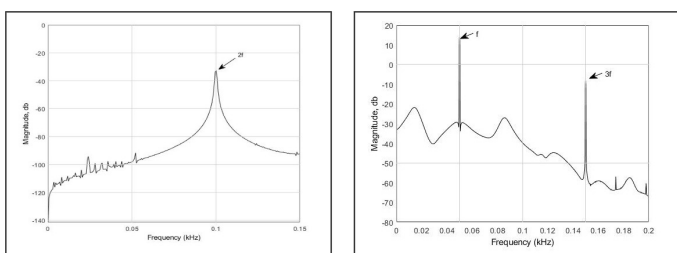


Figure 17. ZCT spectrums for full load condition with 3% grid unbalance and current spectrums for full load condition with 3% grid unbalance

3.4. Network Imbalance and Rotor Failure Modeling and Feature Extraction with Matlab/Simulink

In the Matlab/Simulink model, the network unbalance rate was applied as a constant 3%. The model was created by making one of the rotor resistances 0.205Ω . In the model, the FFT of the ZCT change was calculated and the values in the amplitude of the component were examined. The amplitude variation of the components in the sidebands of the mains frequency was examined by operating the model at quarter, half and full load, and it is seen that the rotor error is in the $2sf$ component of the ZCT signal, and the grid unbalance is in the $2f$ component. In the current signal, it has been observed that the rotor failure is in the $(1-2s)f$ and $(1+2s)f$ components, and the network unbalance is in the $3f$ component. The component amplitudes have no influence on each other in case of rotor failure ($2sf$) when there is a mains unbalance ($2f$) in the motor. In Figure 18, ZCT and current spectrums are seen when the motor is at quarter load, the mains unbalance is 3%, the rotor resistance is increased by 0.205Ω . In Figure 19, ZCT and current spectrums are seen when the motor is at half load, the mains unbalance is 3%, the rotor resistance is increased by 0.205Ω . In Figure 20, the ZCT and current spectrums are seen when the motor is at full load, the mains unbalance is 3%, the rotor resistance is increased by 0.205Ω .

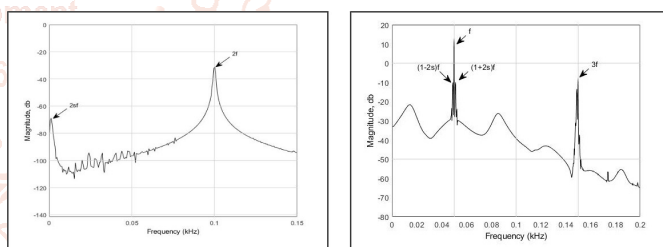


Figure 18. ZCT spectra for quarter load condition when 3% of mains unbalance rotor resistance is 0.205Ω and current spectrums for quarter load condition when rotor resistance is 0.205Ω with 3% mains unbalance

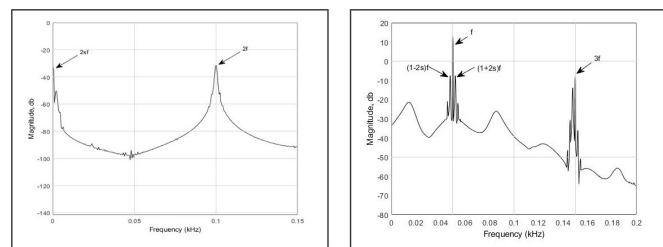


Figure 19. ZCT spectra for half load condition when 3% of mains unbalance rotor resistance is 0.205Ω and current spectrums for half-load condition when the rotor resistance is 0.205Ω with 3% mains unbalance

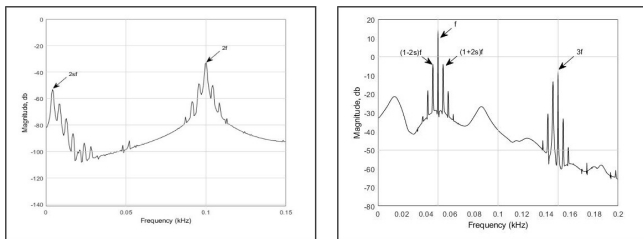


Figure 20. ZCT spectra for full load condition when mains unbalance is 3% rotor resistance 0.205 Ω and current spectrums for full load condition when the rotor resistance is 0.205 Ω with 3% mains unbalance

3.5. Modeling and Feature Extraction of Mechanical Unbalance and Rotor Failure with Matlab/Simulink

In order to create mechanical imbalance in the Matlab/Simulink model, sine of 10% of the actual load is applied in addition to the actual load. For the rotor failure, one of the rotor resistances is made 0.205 Ω and the model is created. In the model, the FFT of the ZCT change was calculated and the values in the amplitude of the component were examined. The amplitude variation of the components in the sidebands of the mains frequency was examined by operating the model at quarter, half and full load, and it is seen that the rotor error is in the 2sf component in the ZCT signal and the mechanical imbalance is in the fr component. In the current signal, it has been observed that the rotor failure is in the (1-2s)f and (1+2s)f components, while the mechanical imbalance is in the (f-fr) and (f+fr) components. In case of rotor failure (2sf) when there is mechanical imbalance (fr) in the motor, the component amplitudes have no influence on each other. Figure 21 shows the ZCT and current spectrums when the rotor resistance is increased by 0.205 Ω at quarter load of the motor (28.19+2.819sin155.5t Nm). In Figure 22, the ZCT and current spectrums are seen when the rotor resistance is increased by 0.205 Ω at half load (55.84+5.584sin153.93t Nm) of the motor. Figure 18 shows the ZCT and current spectrums when the rotor resistance is increased by 0.205 Ω at full load (109.46+10.946sin150.79t Nm).

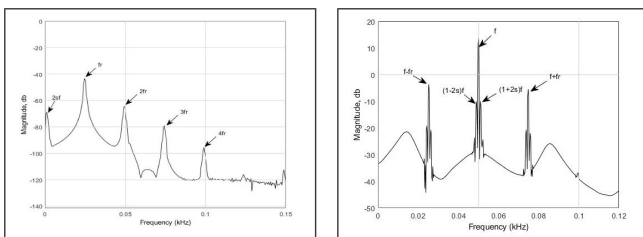


Figure 21. ZCT spectra with motor running at variable quarter load (28.19+2.819sin155.5t Nm) and rotor resistance 0.205 Ω and current spectrums with motor running at variable quarter load (28.19+2.819sin155.5t Nm) and rotor resistance 0.205 Ω

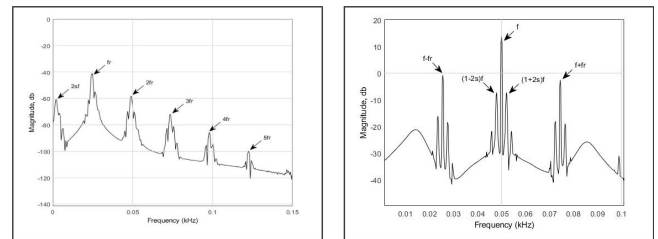


Figure 22. ZCT spectrums with motor running at variable half load (55.84+5.584sin153.93t Nm) and rotor resistance 0.205 Ω and current spectrums with motor running at variable quarter load (55.84+5.584sin153.93t Nm) and rotor resistance 0.205 Ω

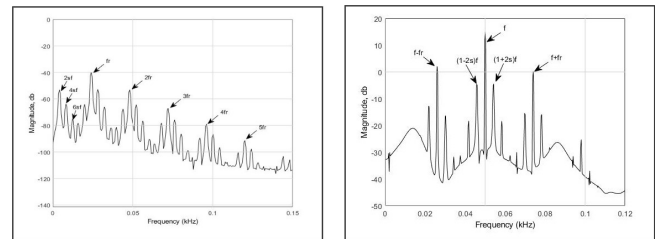


Figure 23. ZCT spectrums with motor running at variable full load (109.46+10.946sin150.79t Nm) and rotor resistance 0.205 Ω and current spectrums with motor running at variable quarter load (109.46+10.946sin150.79t Nm) and rotor resistance 0.205 Ω

3.6. Modeling and Feature Extraction of Mechanical Imbalance and Network Imbalance with Matlab/Simulink

In order to create mechanical imbalance in the Matlab/Simulink model, sine of 10% of the actual load is applied in addition to the actual load. For the grid unbalance, one of the phases is reduced by 3% to create a model. In the model, the FFT of the ZCT change was calculated and the values in the amplitude of the component were examined. By operating the model at quarter, half and full load, the amplitude variation of the components in the sidebands of the mains frequency was examined and it is seen that the mains unbalance is in the 2f component in the ZCT signal, and the mechanical unbalance is in the fr component. In the current signal, it has been observed that the network imbalance is in the 3f component, while the mechanical imbalance is in the (f-fr) and (f+fr) components. In case of mains unbalance (2f) while there is mechanical unbalance (fr) in the motor, the component amplitudes have no effect on each other. In Figure 24, the ZCT and current spectrums of the motor at quarter load (28.19+2,819sin155.5t Nm) at 3% grid unbalance are shown. Figure 25 shows the ZCT and current spectrums when the motor is at half load (55.84+5,584sin153.93t Nm), the grid unbalance is 3%. Figure 26 shows the ZCT and current spectrums when the motor is at full load (109.46+10.946sin150.79t Nm), the grid unbalance is 3%.

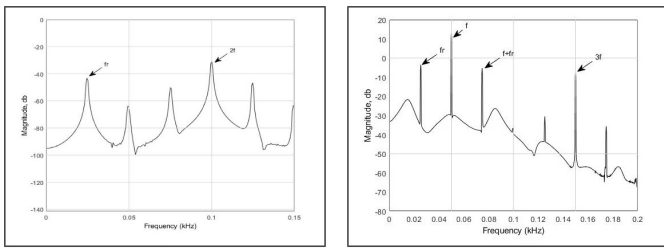


Figure 24. ZCT spectrums with motor running at variable quarter load ($28.19+2.819\sin155.5t$ Nm) and grid unbalance at 3% and current spectrums when the motor is running at variable quarter load ($28.19+2.819\sin155.5t$ Nm) and the mains unbalance is 3%

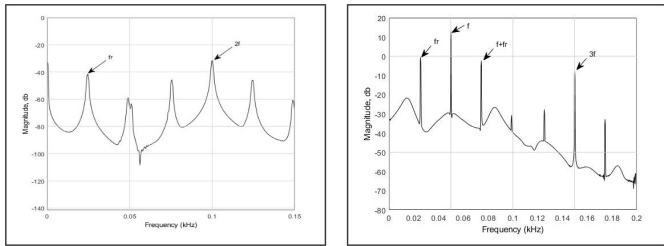


Figure 25. ZCT spectrums when the motor is running at variable half load ($55.84+5.584\sin153.93t$ Nm) and the mains unbalance is 3% and current spectrums when the motor is running at variable half load ($55.84+5.584\sin153.93t$ Nm) and the mains unbalance is 3%

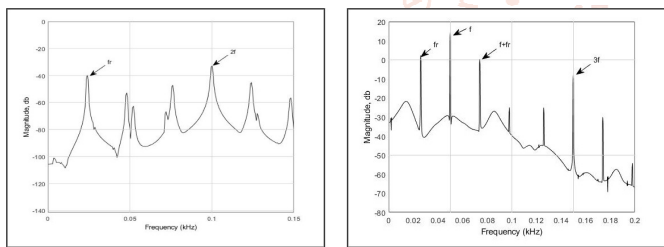


Figure 26. ZCT spectrums with motor running at variable full load ($109.46+10.946\sin150.79t$ Nm) and grid unbalance 3% and current spectrums when the motor is running at variable full load ($109.46+10.946\sin150.79t$ Nm) and the mains unbalance is 3%

3.7. Modeling and Feature Extraction of Mechanical Imbalance Network Imbalance and Rotor Failure with Matlab/Simulink

In the Matlab/Simulink model, in addition to the main load, 10% of the sine of the main load was applied in order to create mechanical imbalance in the Matlab/Simulink model, one of the phases was decreased by 3% for the mains unbalance, and one of the rotor resistances was increased by 205Ω for the rotor failure. In the case of 3 different faults in the model at the same time, the FFT of the ZCT change was calculated and the values in the amplitude of the component were examined. By operating the model at quarter, half and full load, the amplitude changes of the components in the sidebands of the mains

frequency were examined and it is seen that the mains unbalance is in the 2f component in the ZCT signal, the mechanical unbalance is in the fr component, and the rotor failure is in the 2sf component. In the current signal, it was observed that the mains unbalance is in the 3f component, the mechanical unbalance is in the (f-fr) and (f+fr) components, the rotor failure is in the (1-2s)f and (1+2s)f components. If there is a mechanical imbalance (fr) in the motor and a mains imbalance (2f) occurs at the same time as the 3rd fault, which is the rotor fault, the component amplitudes do not have any effect on each other, faults can be distinguished. Figure 27 shows the ZCT and current spectrums of the motor at quarter load ($28.19+2.819\sin155.5t$ Nm), the mains unbalance is 3% and the rotor resistance is 0.205 Ω. Figure 28 shows the ZCT and current spectrums when the motor is at half load ($55.84+5.584\sin153.93t$ Nm), the mains unbalance is 3% and the rotor resistance is 0.205 Ω. Figure 29 shows the ZCT and current spectrums when the motor is at full load ($109.46+10.946\sin150.79t$ Nm), the mains unbalance is 3% and the rotor resistance is 0.205 Ω.

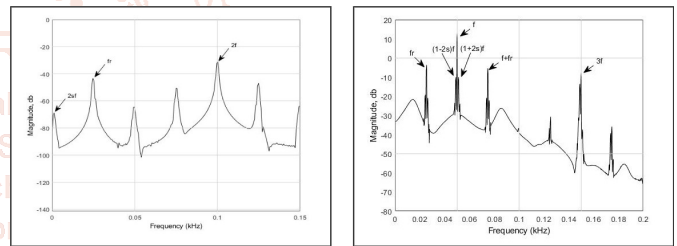


Figure 27. ZCT spectrums with motor running at variable quarter load ($28.19+2.819\sin155.5t$ Nm), mains unbalance 3% and rotor resistance 0.205 Ω and current spectrums when the motor is running at variable quarter load ($28.19+2.819\sin155.5t$ Nm) and the mains unbalance is 3% and the rotor resistance is 0.205 Ω

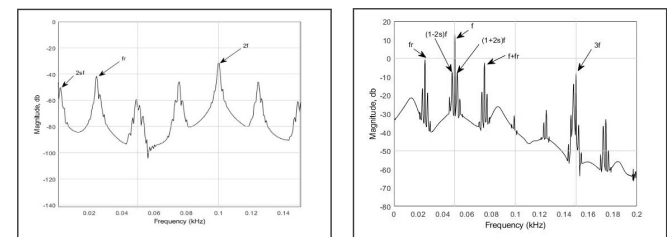


Figure 28. ZCT spectrums with motor running at variable half load ($55.84+5.584\sin153.93t$ Nm) and mains unbalance 3% and rotor resistance 0.205 Ω and current spectrums when the motor is running at variable half load ($55.84+5.584\sin153.93t$ Nm) and the mains unbalance is 3% and the rotor resistance is 0.205 Ω

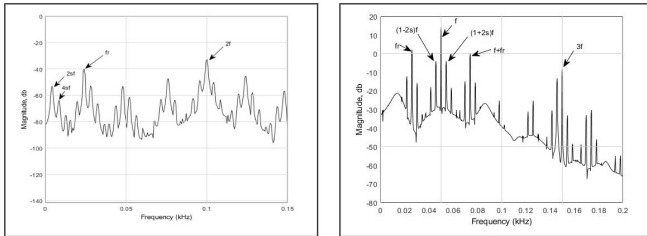


Figure 29. ZCT spectrums with motor running at variable full load ($109.46+10.946\sin150.79t$ Nm) and grid unbalance 3% and current spectrums when the motor is running at variable full load ($109.46+10.946\sin150.79t$ Nm) and the mains unbalance is 3% and the rotor resistance is 0.205Ω

4. CONCLUSIONS

In this study; In the fault detection of induction motors, rotor failure, mechanical unbalance (variable load) failure and mains unbalance fault, also mains unbalance and rotor fault, mechanical unbalance and rotor fault, mechanical unbalance and mains unbalance, mechanical unbalance network unbalance and rotor fault are examined together. Detection of these faults was carried out using ZCT signal in Matlab/Simulink environment.

In addition, it is thought that this application developed can be used for educational purposes for students studying in the field of induction motors. Students using this application will observe what kind of changes are caused by the failures that may occur in the induction motor. Thus, the places where induction motors, which are used in almost all areas of the industrial sector, including daily life, are used, are an application to be used for educational purposes as well as for fault detection.

5. REFERENCES

[1] Askari, M., Keivani, H., Ganbariyan, M., & Kavehnia, F. (2007). *Induction motors control using Zero-Crossing Times signal of stator currents*. Paper presented at the 2007 42nd International Universities Power Engineering Conference.

- [2] Calis, H., & Caki, E. (2014). LabVIEW based laboratory typed test setup for the determination of induction motor performance characteristics. *Journal of Electrical Engineering and Technology*, 9(6), 1928-1934.
- [3] Çalış, H., & Çakır, A. (2007). Rotor bar fault diagnosis in three phase induction motors by monitoring fluctuations of motor current zero crossing instants. *Electric Power Systems Research*, 77(5-6), 385-392.
- [4] Çalış, H., & Çakır, A. (2008). Experimental study for sensorless broken bar detection in induction motors. *Energy Conversion and Management*, 49(4), 854-862.
- [5] Taleb, B., Debnath, K., & Patterson, D. (2005). Design of a ZCT Inverter for a Brushless DC Motor-Simulation Results. in *AUPEC, Tasmania, Australia*.
- [6] Tao, Z., Xia, P., Huang, Y., Xiao, D., Wuang, Y., Zhong, Z., & Liu, C. (2021). *Induction Motor Fault Diagnosis Based on Multi-Sensor Fusion Under High Noise and Sensor Failure Condition*. Paper presented at the 2021 Global Reliability and Prognostics and Health Management (PHM-Nanjing).
- [7] Tran, T. H., Liang, H., Li, W., & Pham, M. T. (2021). Comparison of Machine Learning Algorithms for Induction Motor Rotor Single Fault Diagnosis using Stator Current Signal. *International Journal of Advanced Trends in Computer Science and Engineering*, 10(3), 1509-1514.
- [8] Ukil, A., Chen, S., & Andenna, A. (2011). Detection of stator short circuit faults in three-phase induction motors using motor current zero crossing instants. *Electric Power Systems Research*, 81(4), 1036-1044.